Measurement of Simulated Debris Removal Rates in an Artificial Root Canal to Optimize Laser-Activated Irrigation Parameters

Matija Jezeršek, [ORCID][1]* **Nejc Lukač,[1] and Matjaž Lukač[2]**
[1]Faculty of Mechanical Engineering, University of Ljubljana, Ljubljana, Slovenia
[2]Jozef Stefan Institute, Ljubljana, Slovenia

Background and Objectives: To compare temporal rates of debris removal from an artificial root canal for three laser-assisted irrigation modalities single-pulse super short pulse (SSP), and two dual-pulse X-SWEEPS and AutoSWEEPS, and for two fiber-tip (FT) geometries flat and radial, and to evaluate the dependence of the debris flushing rate on the delay between the SWEEPS laser pulse pair.
Study Design/Materials and Methods: Laser-assisted irrigation was performed with a pulsed Er:YAG laser operating in single-pulse SSP and dual-pulse SWEEPS laser modalities. The laser energy was delivered to the water-filled model access cavity through a FT with either a flat or radial ending. The X-SWEEPS modality delivered pairs of laser pulses separated by a fixed adjustable delay, while with the AutoSWEEPS modality the delay was automatically and repeatedly swept between 200 and 600 microseconds. The debris removal rate was determined with the use of a digital camera by measuring the rate at which a simulated debris was being flushed out of the artificial root canal.
Results: The simulated debris removal rate of the AutoSWEEPS modality is almost three times higher compared with that of the SSP modality. Further, the flat FT outperforms the radial FT by a factor of more than five in the case of SSP, and by more than 10 with AutoSWEEPS. The X-SWEEPS flushing rate exhibits strong dependence on the delay between the SWEEPS pulse pair, with the highest removal rate measured to be more than seven times higher in comparison with SSP.
Conclusion: Dual-pulse laser irrigation modalities (AutoSWEEPS and X-SWEEPS) exhibit significantly higher simulated debris removal rates in comparison with the standard single-pulse SSP laser-assisted irrigation. As opposed to the previously reported dependence of pressure generation on FT geometry, the flat FT's simulated debris removal rate significantly outperforms the radial FT. © 2020 The Authors. *Lasers in Surgery and Medicine* published by Wiley Periodicals LLC

Key words: laser-activated irrigation; Er:YAG laser; root canal irrigation

INTRODUCTION

Root canal treatments consist of mechanical instrumentation followed by irrigation to facilitate the removal of bacteria, debris, and therapeutic materials such as gutta-percha, sealer, and medicaments from root canals [1–3]. While the effectiveness of irrigation relies on both the ability of irrigants to dissolve tissue and the mechanical flushing action to remove material from the canal, it has been suggested that the flushing action is more important than the ability to dissolve tissue, especially since most of the dentine is inorganic matter that cannot be dissolved by sodium hypochlorite (NaOCl) solution [4,5].

The flushing action of the standard syringe irrigation by hand has been found not to be sufficient for removing debris from the root canal [5,6]. For this reason, various other techniques such as negative pressure irrigation [7,8], ultrasonics [9–13], and laser-activated irrigation (LAI) [14–20], have been introduced to enhance the flushing action of irrigant.

The LAI principle is based on rapid vapor bubble generation at the end of a fiber tip (FT) when highly absorbed, pulsed Erbium laser energy (with a wavelength of about 3 μm) is introduced through the FT into the irrigant-filled root canal access opening [21,22]. An example of LAI is photon-induced photoacoustic streaming, performed by a single Er:YAG laser super short pulse (SSP) with duration of 50 microseconds [17,19,23]. One of the advantages of the LAI technique is that the flushing action is not limited to the vicinity of the treatment tip, as is the case with ultrasonic irrigation, but is induced also at distant regions of the canal system [24]. This is because during the life cycle of the vapor bubble, during which the bubble expands and collapses with the bubble oscillation

time (T_B), secondary cavitation bubbles are induced along the entire canal system [14,25,26] that trigger a highly dynamic fluid movement, leading to improved chemo-mechanical debridement [22,24].

The latest LAI development is the SWEEPS™ (Shock Wave Enhanced Emission Photoacoustic Streaming) laser modality, which is based on the delivery of pairs of Er:YAG laser pulses, timed in such a manner to generate enhanced irrigant streaming and shock wave emission, which otherwise occurs only in a free water environment [25–28]. When properly timed, the second pulse within the SWEEPS laser pulse pair accelerates the collapse of the first pulse's primary and secondary bubbles, which induces shock wave emission [25,26] and consequently higher shear forces between the irrigant and canal surface. When the temporal separation (T_p) between the two SWEEPS laser pulses is fixed using the "X-SWEEPS" modality, the largest enhancement of shock waves and internal irrigant pressures occurs when T_p does not deviate substantially from the optimal separation time (T_{opt}), corresponding to the time when the second laser pulse of the X-SWEEPS pulse pair is delivered near the end of the collapse phase of the primary bubble generated by the first laser pulse ($T_{opt} \approx T_B$) [25,26,29].

When using X-SWEEPS modality in clinical practice, it is important to consider that the bubble oscillation time (T_B) depends, among other parameters, on the diameter of the cavity [25,30], and that the dimensions of the access cavity vary from tooth to tooth. Therefore, the X-SWEEPS modality requires the practitioner to adjust the X-SWEEPS pulse separation T_p to the dimension of the access cavity in order to obtain consistent enhancement. As an improved solution, a special AutoSWEEPS Er:YAG laser modality was developed [26,29,31], where the temporal separation between the pair of laser pulses is continuously swept back and forth between $T_p = 200$ and $T_p = 650$ microseconds. This ensures that during each sweeping cycle there is always at least a 50 microseconds wide temporal separation range when the pulses are separated by $T_p \approx T_{opt}$, as required for optimal enhancement. The sweeping modality also ensures that the optimal conditions are approximately reached along the depth of the access cavity by matching the changing diameter conditions during the AutoSWEEPS cycle. The AutoSWEEPS modality also eliminates the need for the operator to precisely position the FT in the center of the cross-section of the root canal.

Under comparable conditions, the AutoSWEEPS modality has been reported to be about 50% more effective than standard SSP in generating pressures within the root canal, signifying about 50% better penetration of irrigants into dentinal tubules [. Also, in a recent study [32], the efficacy of the removal of accumulated hard-tissue debris from the root canal system for the AutoSWEEPS irrigation was compared with the SSP laser-assisted irrigation as well as with ultrasonically activated irrigation (UAI) using microcomputed tomography. The AutoSWEEPS modality resulted in significantly improved debris removal in each portion of the root canals compared with SSP and UAI.

In this study, we investigated the dependence of the flushing rate, that is, the temporal rate of simulated debris consisting of a dentifrice paste, from an artificial root canal model, on the pulse delay T_p of the X-SWEEPS modality, and compared it with the flushing rates obtained with the dual-pulse AutoSWEEPS and single-pulse SSP modality.

MATERIALS AND METHODS

Experimental Setup

The experimental setup for measuring the simulated debris removal rate is presented in Figure 1a. The artificial root canal, made from transparent plexi-glass, was submerged 4 mm deep into a water reservoir in order to ensure the constant replenishment of irrigant, as is in a clinical setting typically performed by an assistant using a syringe. The model had a conically shaped access cavity and a cylindrically shaped canal with diameter $d = 0.8$ mm and length $L = 10$ mm (see Fig. 1b).

The relatively large canal diameter was chosen to ensure repeatable and homogenous filling with simulated debris that was injected into the canal using a medical syringe
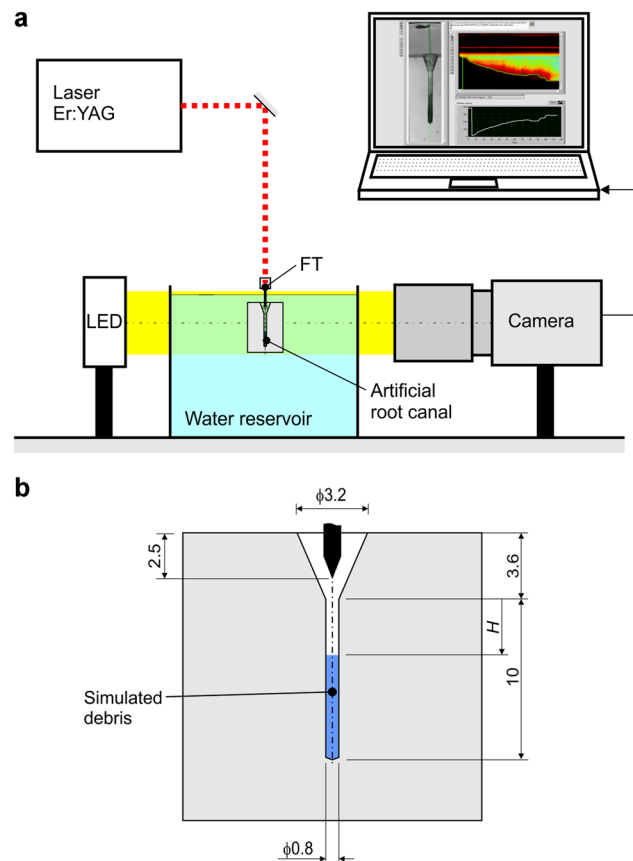
Fig. 1. Experimental system (**a**) where a digital camera captures images of an artificial root canal submerged into water and filled with a simulated debris. The geometry of the root canal model (**b**) is cylindrical with a conical access cavity. The depth of the cleaned out part of the canal (H) is measured from the top of the cylindrical canal.

(0.5 mm diameter) initially positioned at the bottom of the canal. After the whole length L of the canal had been filled-in, the needle was slowly pulled out without stopping the injection in order to ensure the compactness of the simulated debris, and to prevent any formation of empty voids. The homogeneity of the filling was carefully checked each time with a camera. The conical access cavity was cleaned mechanically before each measurement. In preliminary experiments, we tested also the irrigation of a narrower canal ($d = 0.45$ mm), with similar but less reproducible relative results since in this case, the filling had to be made with the syringe positioned at the canal's entrance.

Before each measurement, the artificial root canal was filled with a dental paste (Sensodyne Rapid Relief; GlaxoSmithKline (Brentford, United Kingdom), main ingredients glycerin, PEG-8 isostearate, hydrated silica, and pentasodium triphosphate) to simulate accumulated debris. Initially, we used also a wet sand-like mixture of dentine debris and 2% NaOCl, as is typically used to simulate debris [9,10,33], in addition to the dental paste. However, after preliminary tests using both types of simulated debris, we chose the dental paste in further experiments since results were comparable, and the preparation procedure using the paste was faster and more reproducible.

The simulated debris removal rate was measured with a digital camera (Chameleon3, 1.3 MP; Point Grey Research Inc., Richmond, Canada), which acquired 10 images per second with spatial resolution of 20 μm. A back-illumination with a high-brightness white LED panel (EMOS SI, Polzela, Slovenia)(6 W, 120×120 mm, ZD2122; EMOS SI, Slovenia) was used to achieve good contrast between the filled and cleaned part of the root canal. Custom software was developed for automatic detection of the border between the filled and cleaned part of the canal on every image. The simulated debris removal rate Rd (in mm^3/s) was then calculated as:

$$Rd = H\pi d^2/4\Delta t \tag{1}$$

where H (in mm) is the depth of the cleaned out part of the canal, and Δt (in s) is the observation time period. The observation period was maximally 250 seconds long or equal to the time when the canal became fully flushed out ($H = L$).

This experimental setup measured the removal rate of the bulk material by detecting the overall light intensity passing thought the artificial canal, and was not sensitive enough to detect the cleanliness of the walls, that is, any thin film of the paste potentially remaining on the canal walls.

Laser Irrigation

Laser-assisted irrigation was performed with a pulsed Er: YAG laser (Fotona d.o.o., Ljubljana, Slovenia) ($\lambda = 2.940$ μm) (LightWalker AT; Fotona d.o.o., Slovenia). The laser was equipped with a dental handpiece (H14; Fotona d.o.o.) optically coupled with an interchangeable FT.

Two FT geometries were used in the study (i) a cylindrical flat-ended FT with a diameter of 400 μm (Fotona Flat Sweeps400 tip) and (ii) a cylindrical radially-ended (tapered) tip with a diameter of 400 μm (Fotona Radial Sweeps400 tip). The FT's ending was for all measurements positioned 2.5 mm deep into the access cavity, using an XYZ micrometer positioning stage and the camera with an optical resolution of 20 μm.

Three laser modalities were compared (i) Single-pulse SSP modality; (ii) Dual-pulse X-SWEEPS modality with a fixed adjustable delay T_p between the pulses; and (iii) Dual-pulse AutoSWEEPS modality with the delay T_p being automatically and continuously swept between 200 and 600 microseconds. The SSP pulse duration was 50 microseconds, and the duration of the SWEEPS pulses was 25 microseconds. The SSP laser pulse energy as well as the sum of the energies of the two SWEEPS pulses was 20 mJ. All three modalities were delivered at the pulse repetition rate of 20 Hz.

In the first set of experiments, we compared the flat and radial FT geometries using the SSP and AutoSWEEPS modalities.

In the second set of experiments, we studied the influence of the delay between the two SWEEPS pulses using the X-SWEEPS modality. The fixed delay was varied between 250 and 600 microseconds with 50 microseconds increments. A Flat Sweeps400 FT was used.

In the last experiment, we studied the effect of laser pulse repetition rate on removal rate, where we used SSP modality with pulse energy of 20 mJ. A flat-ended FT with 400 μm diameter was used. This experiment was made to evaluate how much is the removal rate of the double-pulse SWEEPS modality increased just because of the doubled pulse repetition rate in comparison with the single-pulse SSP modality.

Statistical Analysis

In all experiments, at least seven measurements were made for each group. Average values and standard deviations were then calculated and presented in the results. Measured simulated debris removal rates were compared between groups using a one-way analysis of variance (ANOVA) followed by least significant difference multiple comparisons. The level of significance was $P < 0.05$.

RESULTS

The dependence of the simulated debris removal rate on FT geometry for SSP and AutoSWEEPS modalities is shown in Figure 2. The simulated debris removal rate of the AutoSWEEPS modality is almost three times higher compared with that of the SSP modality in case of FT Flat Sweeps400 (0.0076 ± 0.0030 vs. 0.021 ± 0.0033 mm^3/s, $P < 0.00001$). Further, the flat FT outperforms the radial FT by a factor of more than five in the case of SSP (0.0076 ± 0.0030 vs. 0.0016 ± 0.00079 mm^3/s, $P < 0.002$), and by more than 10 with AutoSWEEPS (0.021 ± 0.0033 vs. 0.0024 ± 0.00032 mm^3/s, $P < 0.00001$).

Figure 3 shows the dependence of the simulated debris removal rate on the X-SWEEPS pulse delay. A strong correlation was observed, with the removal rate significantly
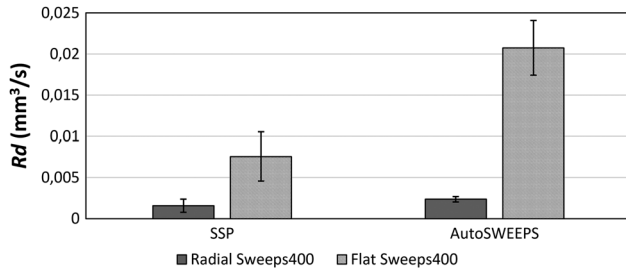
Fig. 2. Simulated debris removal rate dependence on laser modality and FT geometry. FT, fiber-tip; SSP, super short pulse.

higher at longer delays (see the linear fit on Fig. 3; $R^2 = 0.87$).

Figure 4 shows the dependence of the measured depth of cleaning (H) following 250 seconds of irrigation. The entire canal was cleaned ($H = L$) for delays longer than 450 microseconds. The depth of cleaning (H) was significantly lower at shorter delays ($P < 0.011$).

Figure 5 shows the dependence of the simulated debris removal rate on laser modality. There was a statistically significant difference between groups as determined by one-way ANOVA ($F(2,18) = 67.03$, $P < 0.0001$). The highest removal rate was achieved with X-SWEEPS at $T_p = 600$ microseconds ($Rd = 0.061 \pm 0.015$ mm^3/s), followed by AutoSWEEPS (0.021 ± 0.003 mm^3/s), with the considerably smallest removal rate measured for SSP (0.008 ± 0.003 mm^3/s).

Figure 6 compares the flushing efficacy (Fe) defined as $Fe = 100\% \times H/L$, where H is the final depth of cleaning following 250 seconds of LAI for the three tested laser modalities. A complete cleaning ($H = L = 10$ mm) was achieved with X-SWEEPS (in 82 ± 19 seconds) as well as with AutoSWEEPS (in 237 ± 8 seconds), while for SSP the final depth stopped at $H = 4.4 \pm 1.3$ mm, which is significantly less effective compared with either of the double-pulse modalities ($P < 0.0001$).

Finally, Figure 7 shows the influence of the laser pulse repetition rate on the removal rate of the simulated debris, where the single-pulse SSP modality with pulse energy of 20 mJ was used.
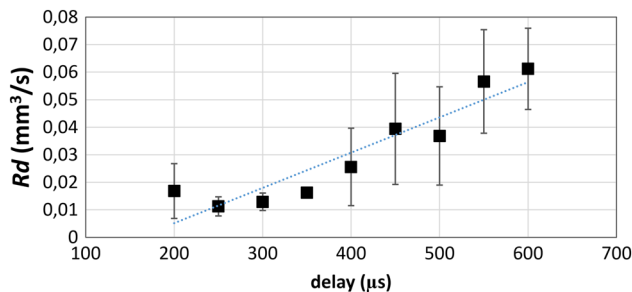

Fig. 3. Dependence of the simulated debris removal rate on SWEEPS delay T_p. The double pulse X-SWEEPS modality was used with a flat-ended fiber tip with 400 μm diameter and combined pulse energy of 20 mJ at a repetition rate of 20 Hz. Linear fit shows a positive correlation between the delay and simulated debris removal rate ($R^2 = 0.87$).
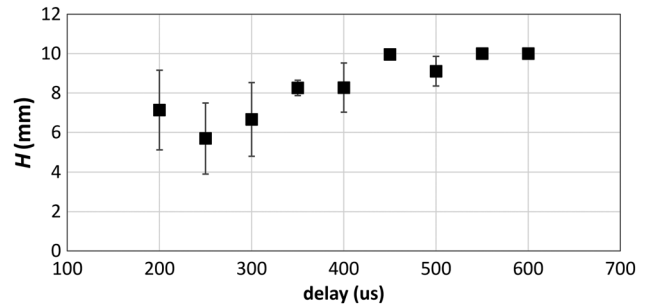

Fig. 4. Dependence of the depth of cleaning H following 250 seconds of irrigation on the SWEEPS pulse delay. The double pulse X-SWEEPS modality was used with a flat-ended fiber tip with 400 μm diameter and combined pulse energy of 20 mJ at a repetition rate of 20 Hz.

DISCUSSION

This *in vitro* study compared the efficacy of three different laser activation techniques on the removal of simulated debris from an artificial root canal using camera imaging of the depth of the canal's cleaning. The removal of hard-tissue debris has been assessed using a number of different methods, including camera imaging [9,10,33], scanning electron microscopy [34], histology [35], and micro-computed tomography [32]. In this study, we used a relatively simple artificial root canal model and a different camera imaging method than typically used, in order to be able to evaluate not only the amount of the remaining simulated debris but also the rate of removal. Our initial tests were made on a more realistic model, which included also several lateral canals. However, this setting resulted in a larger variance of results, where the main reason was less repeatable removal and refilling of the canals following each measurement. Since the lateral canals, located at different depths of the main canal, were observed to get cleaned at about the same rate as the main canal, we decided for the simpler model in order to be able to make a more standardized and consistent comparison of various irrigation rates. For the same reason, that is, to more consistently determine irrigation rates from the achieved cleaning depths, a cylindrical and not a conically shaped root canal model was used. While it is expected that the flushing times will be longer for more
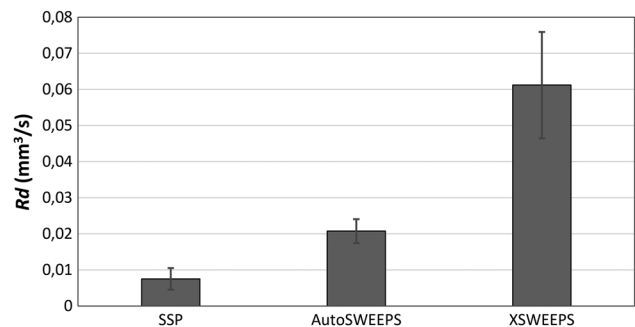

Fig. 5. Simulated debris removal rate measured for different laser modalities. SSP, super short pulse.
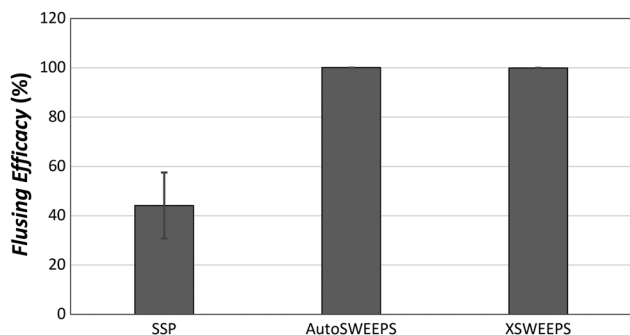
Fig. 6. Flushing efficacy of the SSP, AutoSWEEPS, and X-SWEEPS laser-activated irrigation. SSP, super short pulse.

complex and deeper root canal geometries due to higher friction and longer net length of the entire canal system, we believe that the relative cleaning rates of different laser modalities as observed with our experimental set-up are relevant also for the clinical setting.

Although the injected dental paste is water-based, hydrophilic, and designed to break down into its components with water, while endodontic debris like dentine shavings, soft tissue remnants, and endodontic biofilms will not break down and be disrupted as easily; we believe the measured relative removal rates between different laser irrigation modalities as obtained with the dental paste demonstrate a fundamental difference in the dynamics of photoacoustic streaming depending on the modality used, and are thus relevant also for the actual clinical conditions. The relevance was tested during our initial measurements where we used a simulated debris mixture prepared according to the already accepted recipe described in [9,10,33]. One of the experimental challenges was that both types of the simulated debris started to solidify during the experiment. When dental paste was used, the gradual solidification was slower. Since the initial experiments showed the difference in irrigation rates using either the dental paste or the debris mixture to be less than 20%, we decided to use the dental paste in
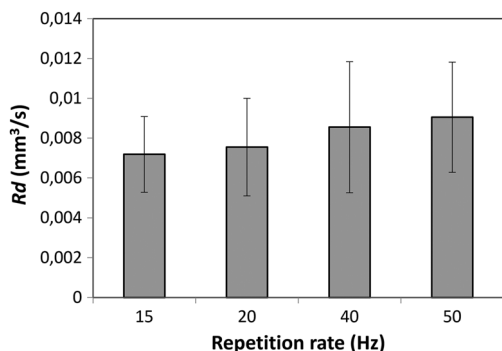

Fig. 7. Influence of the pulse repetition rate of the single-pulse super short pulse modality with pulse energy of 20 mJ on the simulated debris removal rate. A flat-ended fiber tip with 400 µm diameter was used.

further measurements in order to make the experiment more reliable and reproducible.

The irrigation results indicate that the dual-pulse SWEEPS modality is significantly more effective in simulated debris removal in comparison with the already very effective single-pulse SSP modality [24]. Since for the same modality repetition rate, the combined pulse repetition rate of SWEEPS is double that of SSP, the observed enhanced removal rate could at least in principle be caused by the higher pulse repetition rate. However, our measurements of the simulated debris removal rate for the single-pulse SSP modality at different pulse repetition rates (see Fig. 7) demonstrate that this is not the case. The increased pulse repetition rate has only a minor effect on Rd.

As can be seen from Figure 5, the dual-pulse AutoSWEEPS modality outperforms the single-pulse SSP by almost a factor of 3, while at the measured maximal rate the X-SWEEPS modality was more than 7 times more effective than SSP. It is to be noted that while the X-SWEEPS modality achieved three times higher removal rate compared with AutoSWEEPS, its performance strongly depends on the chosen time delay of the second pulse. For optimal flushing rate, the X-SWEEPS delay must approximately match the bubble oscillation time that varies depending on the treated root canal geometry [30]. When during clinical procedures no feedback or other method is available to optimize the pulse delay for particular tooth geometry, the AutoSWEEPS modality represents a more robust and preferable choice. This is because AutoSWEEPS does not require the practitioner to adjust the delay time to the dimensions of the treated root canal. Additionally, it should be noted that the maximal X-SWEEPS rate was not observed at T_p being slightly shorter than T_B, as is the condition for shock wave generation and enhancement of pressure waves [25,26]. Under the conditions used in this study, the measured bubble oscillation time was between 500 and 550 microseconds, while the simulated debris removal rate measurement (see Fig. 3) indicates that the maximal rate occurs at a delay longer than T_B. This is in agreement with another report where the most effective debris removal was observed when the temporal separation between the SWEEPS pulse pair was approximately 50 microseconds longer than the bubble oscillation time [26]. This indicates that due to the complex photoacoustic dynamics during dual-pulse irrigation, different activation mechanisms might not have exactly the same "resonant" SWEEPS pulse pair separation. In this regard, the "auto-sweeping" AutoSWEEPS modality has an additional advantage since it achieves optimal pulse separations for different activation mechanisms at least twice during every sweeping cycle.

Our measurements also show that for simulated debris removal, the flat FT significantly outperforms the radial FT. Although the observed difference in effectiveness of the two FT types may be at least partially a consequence of the particular experimental setup used, we believe that the observed difference may of relevance for *in vivo* cases. As has been observed using fast camera imaging [26],

there is a difference between bubble dynamics for flat and radials tips. When using a flat tip the subsequent bubble from the second laser pulse of the SWEEPS pair is observed to effectively "propel" the initial bubble deeper into the canal, thus potentially improving the irrigation effect deeper within the canal. This effect is less pronounced when using a radial tip.

The observed superiority of the flat FT for simulated debris removal is different from what has been measured for internal pressure generation, where the radial FT outperforms the flat FT, except for FT diameters equal to or smaller than 400 μm, where the pressure generation of both FTs becomes approximately the same [24,29,31].

It is important to note that AutoSWEEPS irrigation has not been observed to increase the risk of apical irrigant extrusion. In a study of the apical irrigant extrusion during SSP and AutoSWEEPS laser irrigation [28], a significantly lower rate of apical extrusion compared with the conventional irrigation with endodontic irrigation needles was reported. Similarly, in a recent study of generated pressures during LAI [31], there was no significant difference observed between the measured pressures in the apical area for the SSP and AutoSWEEPS protocols.

CONCLUSIONS

In conclusion, the AutoSWEEPS and X-SWEEPS dual-pulse SWEEPS laser irrigation modalities exhibit significantly higher simulated debris removal rates in comparison with the standard single-pulse SSP laser-assisted irrigation. As opposed to the previously reported dependence of pressure generation on FT geometry, the flat FT's simulated debris removal rate significantly outperforms that of the radial FT.

ACKNOWLEDGMENTS

REFERENCES

1. Peters OA. Current challenges and concepts in the preparation of root canal systems: A review. J Endod 2004;30:559–567.
2. Peters OA, Schonenberger K, Laib A. Effects of four Ni-Ti preparation techniques on root canal geometry assessed by micro computed tomography. Int Endod J 2001;34:221–230.
3. Hulsmann M, Rummelin C, Schafers F. Root canal cleanliness after preparation with different endodontic handpieces and hand instruments: A comparative SEM investigation. J Endod 1997;23:301–306.
4. Baker NA, Eleazer PD, Averbach RE, Seltzer S. Scanning electron microscopic study of the efficacy of various irrigation solutions. J Endod 1975;1:127–135.
5. Walters MJ, Baumgartner JC, Marshall JG. Efficacy of irrigation with rotary instrumentation. J Endod 2002;28:837–839.
6. Chow TW. Mechanical effectiveness of root canal irrigation. J Endod 1983;9:475–479.
7. Li-sha Gu, Jong RK, Junqi Ling, Kyung KC, Pashley DH, Tay FR. Review of contemporary irrigant agitation techniques and devices. J Endod 2010;35(6):791–804.
8. Susin L, Liu Y, Yoon JC, et al. Canal and isthmus debridement efficacies of two irrigant agitation techniques in a closed system. Int Endod J 2010;43(12):1077–1090.
9. Lee SJ, Wu MK, Wesselink PR. The effectiveness of syringe irrigation and ultrasonics to remove debris from simulated irregularities within prepared root canal walls. Int Endod J 2004;37:672–678.
10. Rödig T, Sedghi M, Konietschke F, Lange K, Ziebolz D, Hülsmann M. Efficacy of syringe irrigation, RinsEndo and passive ultrasonic irrigation in removing debris from irregularities in root canals with different apical sizes. Int Endod J 2010;43:581–589.
11. Ahmad M, Pitt Ford TR, Crum LA, Walton AJ. Ultrasonic debridement of root canals: Acoustic cavitation and its relevance. J Endod 1988;14:486–493.
12. Bryce G, MacBeth N, Gulabivala K, Ng YL. The efficacy of supplementary sonic irrigation using the EndoActivator® system determined by removal of a collagen film from an ex vivo model. Int Endod J 2018;51:489–497.
13. Charara K, Friedman S, Sherman A, et al. Assessment of apical extrusion during root canal irrigation with the novel GentleWave system in a simulated apical environment. J Endod 2016;42:135–139.
14. Blanken JW, Verdaasdonk RM. Cavitation as a working mechanism of the Er,Cr:YSGG laser in endodontics: A visualization study. J Oral Laser Appl 2007;7:97–106.
15. De Moor RJ, Blanken J, Meire M, Verdaasdonk R. Laser activated irrigation or cavitation causing laser driven irrigation. Part 2: Evaluation of the efficacy. Lasers Surg Med 2009;41(7):520–523.
16. de Groot SD, Verhaagen B, Versluis M, Wu MK, Wesselink PR, van der Sluis LW. Laser-activated irrigation within root canals: Cleaning efficacy and flow visualization. Int Endod J 2009;42:1077–1083.
17. Koch J, Jaramillo D, DiVito E, Peters O. Irrigant flow during photon-induced photoacoustic streaming (PIPS) using particle image velocimetry (PIV). Clin Oral Invest 2016;20:381–386.
18. Arslan D, Kustarci A. Efficacy of photon-initiated photoacoustic streaming on apically extruded debris with different preparation systems in curved canals. Int Endod J 2018;51:e65–e72.
19. Olivi G, DiVito E. Photoacoustic endodontics using PIPS™: Experimental background and clinical protocol. LAHA 2012. 22–25.
20. Matsumoto H, Yoshimine Y, Akamine A. Visualization of irrigant flow and cavitation induced by Er:YAG laser within a root canal model. J Endod 2011;37:839–843.
21. Gregorcic P, Jezersek M, Mozina J. Optodynamic energy-conversion efficiency during an Er:YAG-laser-pulse delivery into a liquid through different fiber-tip geometries. J Biomed Opt 2012;17:075006.
22. Lukac N, Zadravec J, Gregorcic P, Lukac M, Jezersek M. Wavelength dependence of photon-induced photoacoustic streaming technique for root canal irrigation. J Biomed Opt 2016;21:75007.
23. Lukac M, Pustovrh G. Modeling modeling photoacoustic efficiency during erbium laser endodontics. J Laser Health Acad 2013;2013(2):1–7.
24. Lukac N, Gregorcic P, Jezersek M. Optodynamic phenomena during laser-activated irrigation within root canals. Int J Thermophys 2016;37:66.
25. Lukac N, Jezersek M. Amplification of pressure waves in laser-assisted endodontics with synchronized delivery of Er:YAG laser pulses. Lasers Med Sci 2018;33(4):823–833.
26. Lukac N, Tasic Muc B, Jezersek M, Lukac M. Photoacoustic endodontics using the novel SWEEPS Er:YAG laser modality. J LAHA 2017;2017:1–7.
27. Gregorcic P, Jamsek M, Lukac M, Mozina J, Jezersek M. Synchronized delivery of Er:YAG-laser-pulse energy during oscillations of vapor bubbles. LAHA 2014;17:14–19.
28. Jezersek M, Jereb T, Lukac N, Tenyi A, Lukac M, Fidler A. Evaluation of apical extrusion during novel Er:YAG laser-activated irrigation modality. Photobiomodul Photomed Laser Surg 2019;37:544–550.
29. Ivanusic T, Lukac M, Lukac N, Jezersek M. SSP/SWEEPS endodontics with the SkyPulse Er:YAG dental laser. J LAHA 2019;2019(1):1–10.

30. Lukac M, Lukac N, Jezersek M. Characteristics of bubble oscillations during laser-activated irrigation of root canals and method of improvement [published online ahead of print February 17, 2020]. Lasers Surg Med 2020. https://doi.org/10.1002/lsm.23226

31. Jezeršek M, Lukac N, Lukac M, Tenyi A, Olivi G, Fidler A. Measurement of pressures generated in root canal during Er:YAG laser-activated irrigation [published online ahead of print June 16, 2020]. Photomed Laser Surg 2020.

32. Yang Q, Liu MW, Zhu LX. Micro-CT study on the removal of accumulated hard-tissue debris from the root canal system of mandibular molars when using a novel laser-activated irrigation approach. Int Endod J 2020;53(4):529–538.

33. Lee SJ, Wu MK, Wesseling PR. The efficacy of ultrasonic irrigation to remove artificially placed dentine debris from different-sized simulated plastic root canals. Int Endod J 2004;37:607–612.

34. Mattioli-Belmonte M, Orsini G, Giuliodori F, et al. Evaluation of an automated system for root canal irrigation: A scanning electron microscopy study. Dent Mater J 2012;31(6):969–974.

35. Neelakantan P, Devaraj S, Jagannathan N. Histologic assessment of debridement of the root canal isthmus of mandibular molars by irrigant activation techniques ex vivo. J Endod 2016;42(8):1268–1272.